PAO-SD : TEST BENCH AND TESTING PROCEDURES FOR PMT XP1805/D1 BASE PRODUCTION

M.Aglietta[1], A.Castellina, W.Fulgione, P.L.Ghia, F.Gomez, C. Morello[1]
Istituto di Fisica dello Spazio Interplanetario del CNR and INFN - Sezione di Torino, Cso Fiume 4, 10133 Torino, Italy

A.Chiavassa, G.Navarra, C.Vigorito
Dipartimento di Fisica Generale dell'Università and INFN - Sezione di Torino, Via P.Giuria,1 10125 Torino, Italy

B. Genolini, T. Nguyen Trung
Institut de Physique Nucléaire d'Orsay, IN2P3-CNRS, Université Paris-Sud Orsay, 91406 Orsay Cedex, France

G. Benettin, A. Pennella
Neohm Componenti, Via Torino, 217, 10040 Leini (To), Italy

Abstract

This document describes the test bench and the testing procedures for an automatic functionality control of the XP1805/D1 photomultiplier bases used in the Surface Detector [1] of the Pierre Auger Observatory. Test bench and testing procedures have been designed by CNR-INFN and IPN groups and developed in collaboration with the Neohm Company. Two identical test benches are currently used at Neohm (Italy) and FEDD (France) to control the PAO bases produced respectively by INFN-Torino and IPN-Orsay. In the following the procedures used to test the bases produced by INFN are discussed together with the results on uniformity of the base pre production.

Keywords: Surface Detector ; Photomultiplier Base.

1. Introduction

An automatic test bench has been developed to control the photomultiplier base [2,3] functionality and to characterize the High Voltage Power Supply (HVPS) response at the end of the production chain. The test bench has been carried out, according to given specifications, by the Neohm company producing the bases for INFN. Two identical test benches are currently used at Neohm and FEDD to control the bases produced respectively by the Torino and Orsay groups. Minor differences exist between the procedures used at Neohm and at FEDD.
For the pre-production performed in 2002 all the HVPS assembled on the bases have been previously fully checked on a dedicated test bench [4], this is, however, not the case for the full production and the HVPS will be completely characterized by the procedure described in the following.
This note illustrates the test bench and the test procedure used by the Torino group. The results obtained by testing the first 73 bases produced in 2002 are also presented and discussed.

2. Test bench overview

The bench is a multi channel configuration including different instruments designed to perform a standard automatic sequence of operations to test the whole base functionalities: high voltage power supply characteristics, dynode voltage repartition, dynode amplifier, coupling capacitors, buffer gain, slow control and coaxial cables.
The system consists of a mechanical holder used to connect the base with spring probes and a separate main control board as shown on fig.1. Relays are used to multiplex the base voltages and signals to the measurement devices and to allow pulse injection on the anode and dynode pins.

[1] Corresponding authors: aglietta@to.infn.it, morello@to.infn.it

The high voltage measurements are performed by the 1000:1 divider (500 MOhm input impedance) implemented on the main board.
The instruments and the electronics components included in the test bench at Neohm are the following:

- HP8116A function generator to simulate the PMT anode output;
- HP8082A pulse generator to simulate the PMT dynode output;
- HP335D (-40 dB attenuator);
- PM6666 counter to measure the RC decaying time of the anode decoupling;
- HP34401A digital multimeter for the low voltages measurements;
- +/- 18 V stabilized power supply
- main control board
- Personal computer
- Digitizing oscilloscope TDS340

Fig. 1 and 2 show the connections between the base and the instruments used in the test. A block diagram of the system is shown on Appendix A. A view of the full system as used at the Neohm company is shown in fig 3.

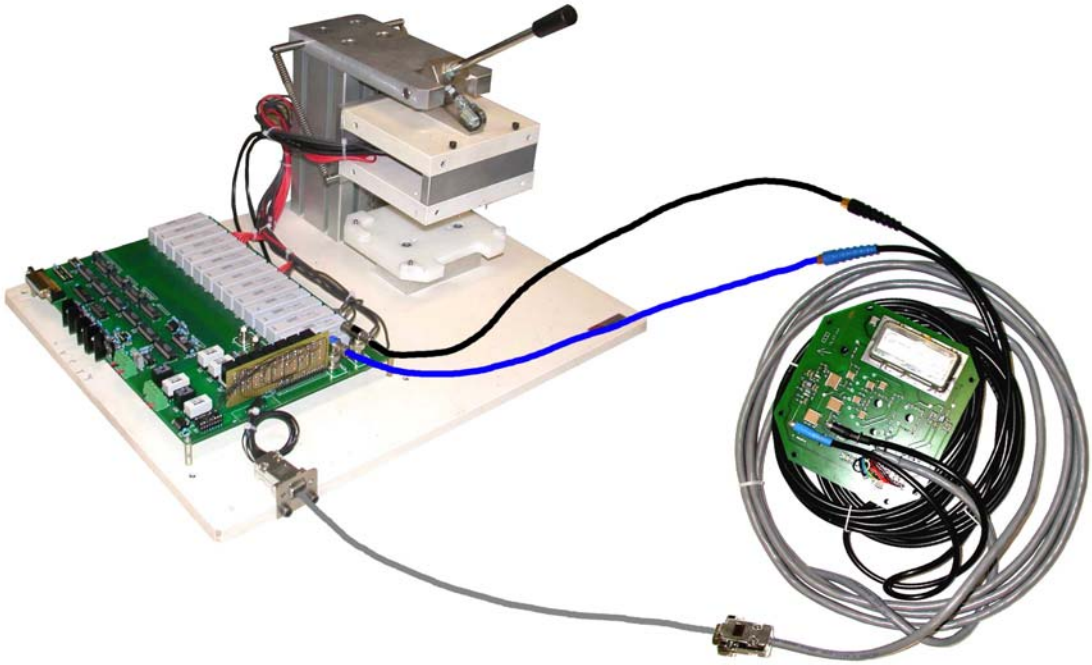

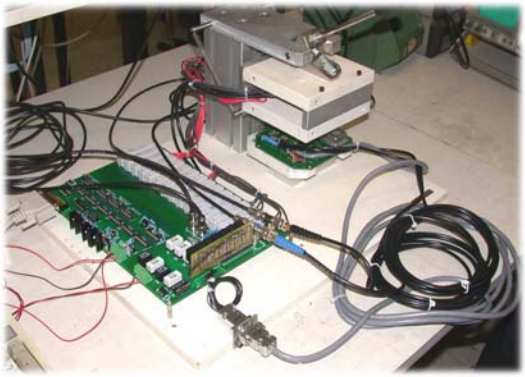

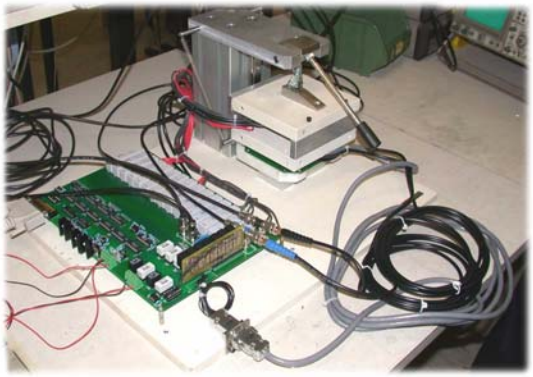

Fig.1

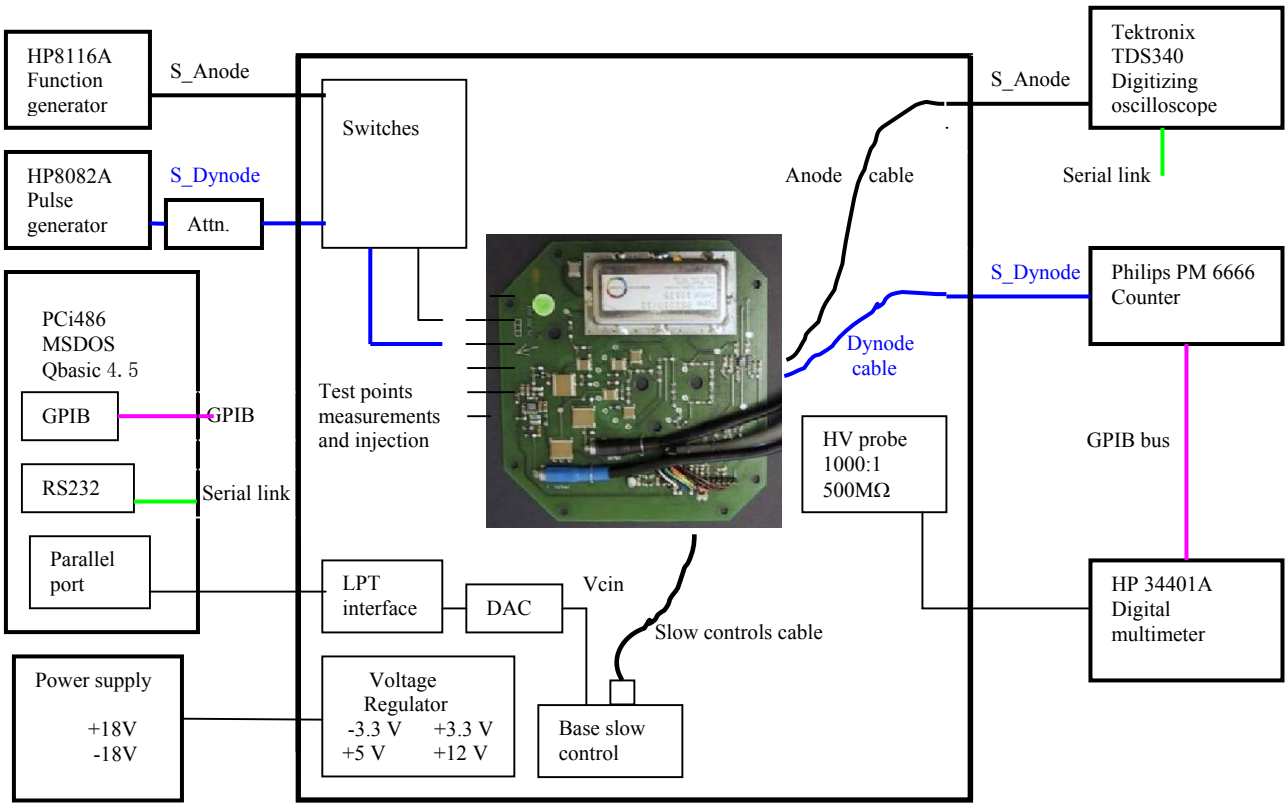
HP8116A
Function
generator
S_Anode
HP8082A
Pulse
generator
S_Dynode
Attn.
Switches
Tektronix
TDS340
Digitizing
oscilloscope
S_Anode
Anode cable
Serial link
S_Dynode
Philips PM 6666
Counter
Dynode
cable
PCi486
MSDOS
Qbasic 4. 5
GPIB
GPIB
RS232
Serial link
Parallel
port
Test points
measurements
and injection
HV probe
1000:1
500MΩ
GPIB bus
LPT
interface
DAC
Vcin
Slow controls cable
HP 34401A
Digital
multimeter
Power supply
+18V
-18V
Voltage
Regulator
-3.3 V +3.3 V
+5 V +12 V
Base slow
control

Fig.2

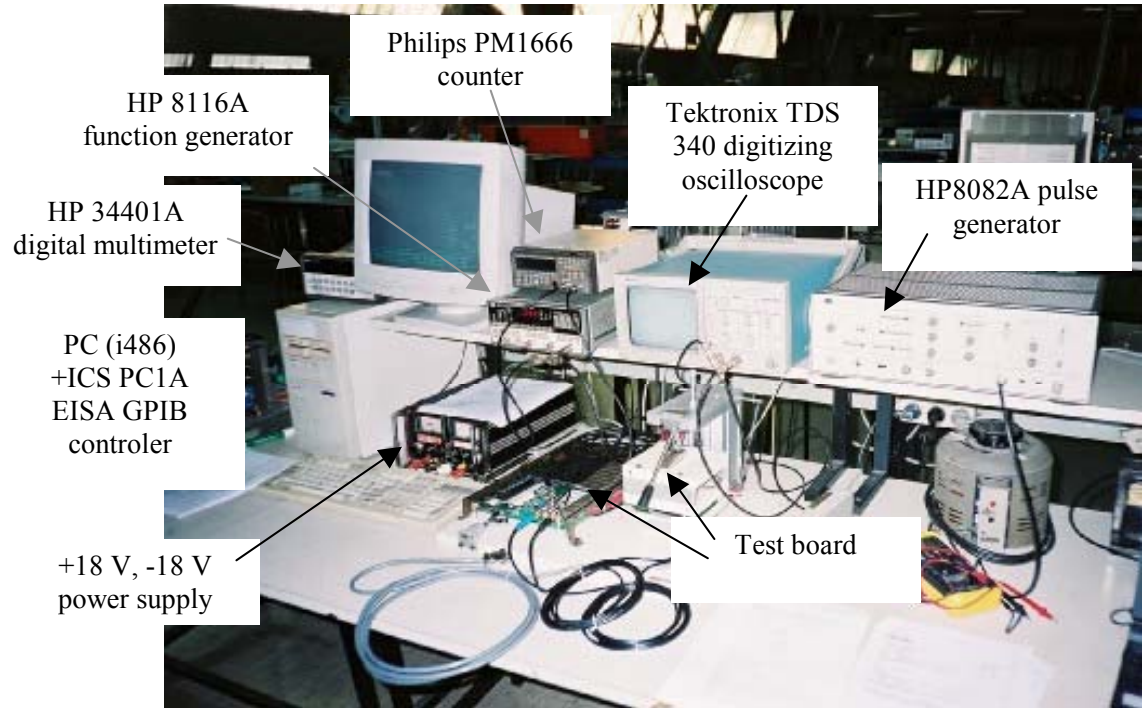
Philips PM1666
counter
HP 8116A
function generator
Tektronix TDS
340 digitizing
oscilloscope
HP8082A pulse
generator
HP 34401A
digital multimeter
PC (i486)
+ICS PC1A
EISA GPIB
controler
+18 V, -18 V
power supply
Test board

Fig.3

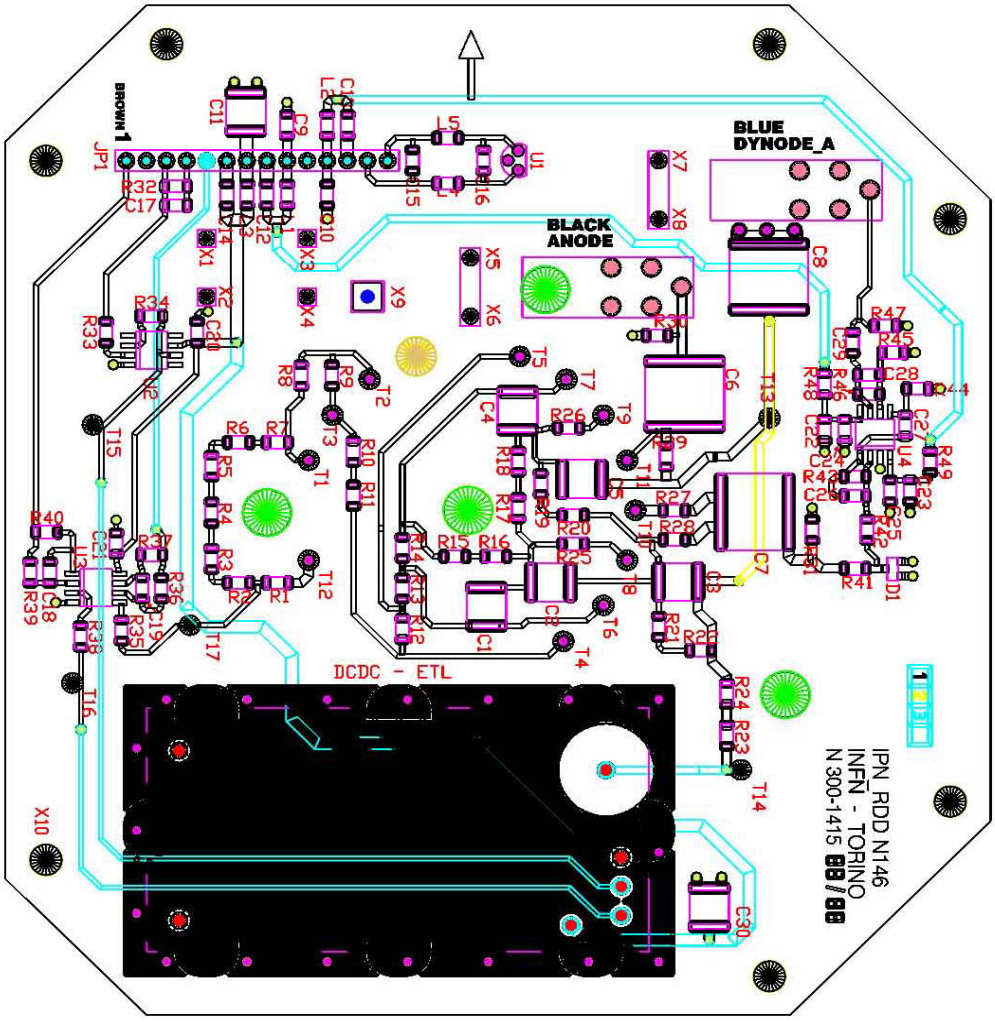

Fig. 4

The electrical parameters of the base are measured through 17 test points (T_1-T_{17}) introduced 'ad hoc' on the printed circuit board as shown on fig. 4. The base electrical drawings including the test points are shown in appendix B: apart from the test points the base layout is the same as in [2,3].
For the bases produced by INFN in 2003 the arrow indicates the proper orientation of the PMT in the Earth's magnetic field [5].

3. Test Procedure

A personal computer connected to the main board via GPIB interface and to TDS340 via RS232 controls and synchronizes the whole procedure: 81 electrical parameters (P_1-P_{81}) are measured and stored as explained in Table 1.
Data for each base are associated to a base serial number (P_0) which is the HVPS serial number so allowing to retrace the base performances at the beginning of its life. The full testing procedures last 5 minutes. Any value of the measured parameters outside given ranges stops the testing procedure.
The procedure is organized in 7 different sections according to Table 1 and it is executed before and after the thermal stress and burn-in process. Some measurements are performed by means of the anode, dynode and slow control cables: by doing so also the cables are tested at the end of the production chain.

Measure		HV setting	Data & Test point	
1	I absorbed on ±3.3V, +12V	Vcin=0	P_1-P_3	
2	HVPS characterization	Vcin from 0.5V to 2.5V in 9 steps	P_4-P_{48}	T_{12}, T_{14}, J_1
3	Divider resistors	Vcin=2.5V	P_{51}-P_{63}	T_1-T_{14}
4	Buffers	Vcin=2.5V	P_{66}-P_{73}	T_{15}-T_{17}
5	Anode decoupling	Vcin=0 Square wave injection	P_{75}	T_{11}, anode cable
6	Dynode amplifier	Vcin=0 Pulse injection	P_{76}-P_{80}	T_{10}, dynode cable
7	Temperature sensor	Vcin=0	P_{81}	J_1

Table 1. List of the sections of the testing procedure. P_1-P_{81} is the raw data sequence of the measurement; T_1-T_{17} the test points for the spring probes; J_1 the slow control connector of the PAO base.

The estimated error for measurements in the range 0-12V is ± 1mV, for the HV measurements ± 1V.

1) The absence of any short circuit and the normal current absorption of the base are tested with the HVPS OFF, i.e. with the voltage command (Vcin) set to 0. For each power line (±3.3V, +12V) the absorbed current is obtained from the ΔV across a 10 Ω series resistor.
2) The HVPS response is fully studied by measuring the HV output (HV), the monitoring voltage (Vmon), the monitoring current (Imon) and the power absorption on 12V power supply for Vcin ranging from 0.5V to 2.5V, 250mV step. A 12 bits DAC (DAC312) on the main board generates the Vcin command. For each step the parameters read out is executed after a settling time of 10 sec according to previous tests [4] (i.e. 10 times the RC time constant on the Vcin input).
Imon is obtained from the voltage measured across R1 (see the electrical drawing of Appendix B). It can therefore be used to obtain the actual voltage used to supply the PMT.
3) The voltage repartition (test points T_1-T_{14}) on the dynodes is measured with an HVPS command Vcin=2.5V corresponding to the nominal HV output of 2000 V. For this purpose all the voltages on the dynodes are multiplexed on the same HV divider 1000:1 ratio (500MΩ over 500KΩ) implemented on the main board.The measured dynode voltages are converted through the proper normalization factor in the corresponding resistance values.
4) Buffers are mounted on each base to interface the slow control signals (Vmon, Vcin and Imon) with the slow control electronics. After setting Vcin=2.5V the gain of the buffers is tested by measuring the voltages before (Vi) and after (Vo) the buffer itself.

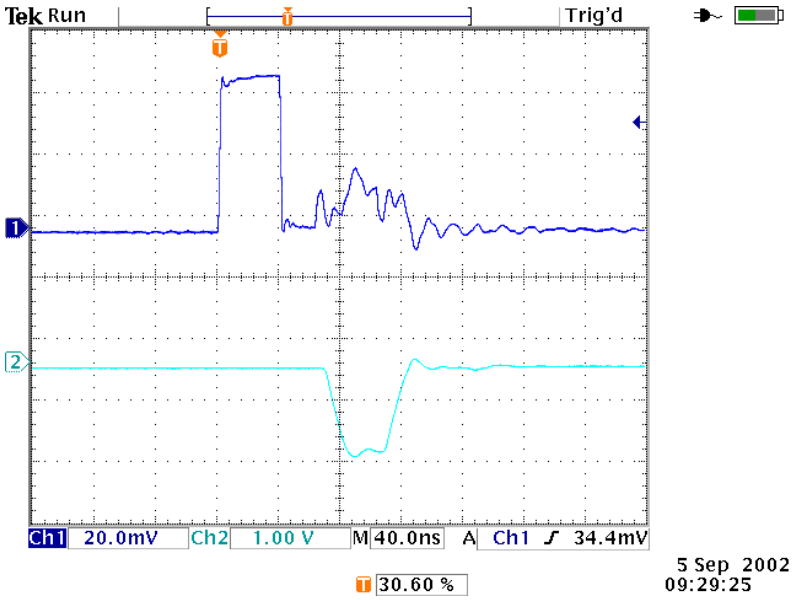

Fig.5. Ch. 1: input signal to the dynode amplifier. The reflection due to the impedance non adaptation is clearly shown. Ch. 2: output signal from the dynode amplifier.

5) Due to the positive polarity used for the PMT high voltage the anode output is decoupled by means of a 10 nF capacitor. To check the value of this capacitor a voltage square wave (width=5ms) generated by the HP8116A is injected on the anode pin connection (T_{11}). The anode output cable is sent on the PM6666 counter (R_{in}=1MΩ) to measure the RC time constant.
6) To check the dynode amplifier a small (50 mV) fast pulse is injected on the last dynode pin connection (T_{10}). As the amplifier input is not adapted to the cable impedance, the pulse width (40ns) and the cable length are chosen such that the main pulse and its reflection are well separated, not to interfere with the amplitude measurements of the signals, as shown on Fig 5.
The dynode output cable is connected to the oscilloscope to measure the amplification factor from the ratio between the output pulse and the input one. At the same time the output pulse fall time gives a simple way to monitor the amplifier bandwidth.
7) The last check is on the temperature sensor. The voltage across a 10kΩ resistor on the main board (the temperature sensitivity is 10mV/K) is read and compared with the room temperature.

4. Thermal Stress

At the end of the production line, each base is submitted to a thermal stress and burn-in process, following the indications reported in [6].
The thermal screening and stress last 24 hours according to the temperature curve shown in fig. 6. During this time the bases are fully supplied (± 3.3V,+12V) with constant HV 2000V (Vcin=2.5V).
There is no voltage monitoring or read-out of electrical parameters during the thermal cycle; however two LEDs on ± 3.3 V and + 12 V lines allow to continuously monitor the base status: all the pre-production bases successfully passed this step. Fig. 7 shows the oven setup used for the thermal stress for the pre-production.

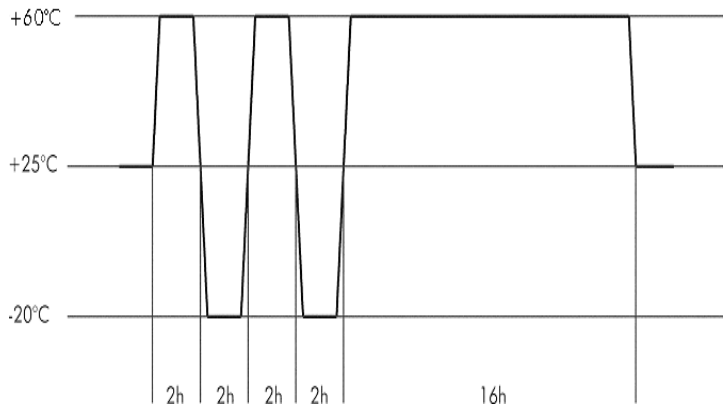

Fig. 6: Thermal Stress Screening and Burn-in cycle

Fig. 7: View of the oven setup for the thermal cycle for the pre production bases

5. Data Analysis

An off-line analysis is performed on the raw data (P1-P81) before delivering the bases. The full data output for one base is summarized in 45 parameters as shown on Tab. 2 and 3. Both the raw data and the given results are stored in Torino to allow future controls in case of failures.

Header	BASE SN 10147 FILE AB190902
D1-D10	1.944 3.384 -3.369 1.000 1.000 1.000 1.225 27.210 29.968 2.968
D11-D20	0.7887 1.9463 4.9081 1.5955 1.5438 0.00871 0.6339 0.8142 0.0356 0.4184
D21-D28	0.1 1759.8 0.3 2261.9 0.2 2008.3 0.4 1971.2
D29-D40	25.00 22.61 20.01 17.81 15.82 14.51 13.39 12.30 9.73 8.85 8.69 0.0501
D41-D45	2.510 4.885 4.009 23.411 2044.1

Tab. 2 : Full data output for one base.

D1	Current 12V [mA]	D24	Vcin value [mV]
D2	Current 3.3V [mA]	D25	Max non-lin diff.(10^{-3}) HV vs Vcin
D3	Current -3.3V [mA]	D26	Vcin value [mV]
D4	Buffer Gain Vcin	D27	Max non-lin diff.(10^{-3}) HV vs Vmon
D5	Buffer Gain Vmon	D28	Vmon value [mV]
D6	Buffer Gain Imon	D29	Anode resistor value [MΩ]
D7	Anode output RC [ms]	D30	Dynode 8 [MΩ]
D8	Gain dynode amplifier	D31	Dynode 7 [MΩ]
D9	Bandwidth dynode amplifier [MHz]	D32	Dynode 6 [MΩ]
D10	Temperature sensor [V]	D33	Dynode 5 [MΩ]
D11	p0 Vmon vs Vcin [mV]	D34	Dynode 4 [MΩ]
D12	p1 Vmon vs Vcin	D35	Dynode 3 [MΩ]
D13	p0 Imon vs Vcin [mV]	D36	Dynode 2 [MΩ]
D14	p1 Imon vs Vcin	D37	Grid 2 [MΩ]
D15	p0 I12 vs Vcin [mV]	D38	Dynode 1 [MΩ]
D16	p1 I12 vs Vcin	D39	Grid 1 [MΩ]
D17	p0 HV vs Vcin [V]	D40	R for Imon output [MΩ]
D18	p1 HV vs Vcin	D41	Vcin max (2500mV) [mV]
D19	p0 HV vs Vmon [V]	D42	Vmon max [mV]
D20	p1 HV vs Vmon	D43	Imon max [mV]
D21	Max non-lin diff.(10^{-3}) Vmon vs Cin	D44	I12 max [mA]
D22	Vcin value [mV]	D45	HV max [V]
D23	Max non-lin diff.(10^{-3}) Imon vs Vcin		

Tab. 3: Parameters list of the off-line analysis

For the pre production a reduced data output has been given to the collaboration as shown on Tab. 4 and 5.

Header	BASE SN 10147 FILE AB190902
D1-D8	0.7887 1.9463 4.9081 1.5955 0.6339 0.8142 0.0356 0.4184
D9-D16	0.1 1759.8 0.3 2261.9 0.2 2008.3 0.4 1971.2

Tab. 4 : The reduced data output

D1	p0 Vmon vs Vcin [mV	D9	Max non-lin diff.(10^{-3}) Vmon vs Vcin
D2	p1 Vmon vs Vcin	D10	Cin value [mV]
D3	p0 Imon vs Vcin [mV]	D11	Max non-lin diff.(10^{-3}) Imon vs Vcin
D4	p1 Imon vs Vcin	D12	Cin value [mV]
D5	p0 HV vs Vcin [V]	D13	Max non-lin diff.(10^{-3}) HV vs Cin
D6	p1 HV vs Vcin	D14	Cin value [mV]
D7	p0 HV vs Vmon [V]	D15	Max non-lin diff.(10^{-3}) HV vs Vmon
D8	p1 HV vs Vmon	D16	Vmon value [mV]

Tab. 5 : Parameters list of the reduced data output

6. Pre-production Results

Fig 8 shows the distributions of the power supply currents measured for the first 73 bases. The values measured on ±3.3V are in good agreement with the AD8012 (dynode amplifier) specifications.

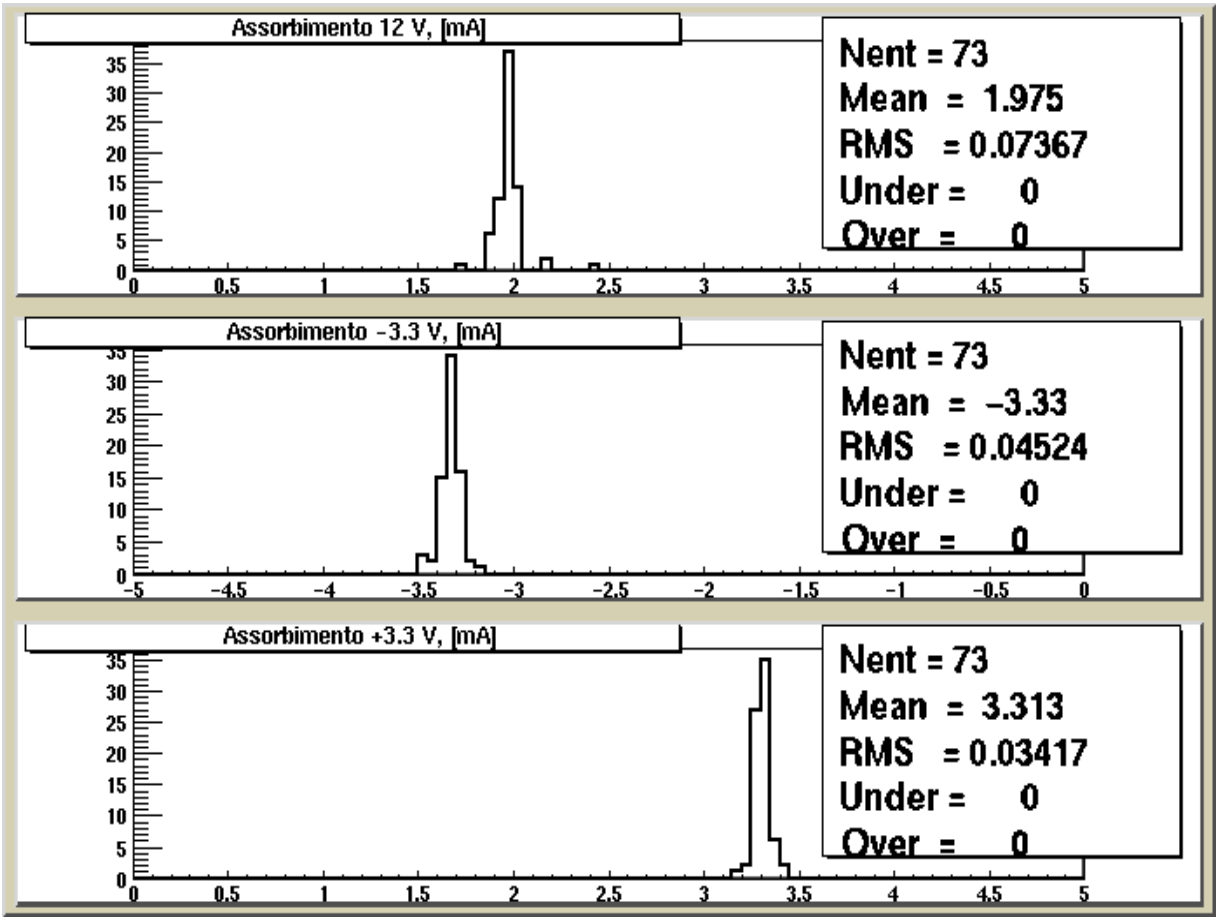

Fig.8

Fig. 9 and 10 show the results of the measurements of the resistor chain. In the histogram titles the expected values are highlighted. All the measured values are within 1% of the expected ones.

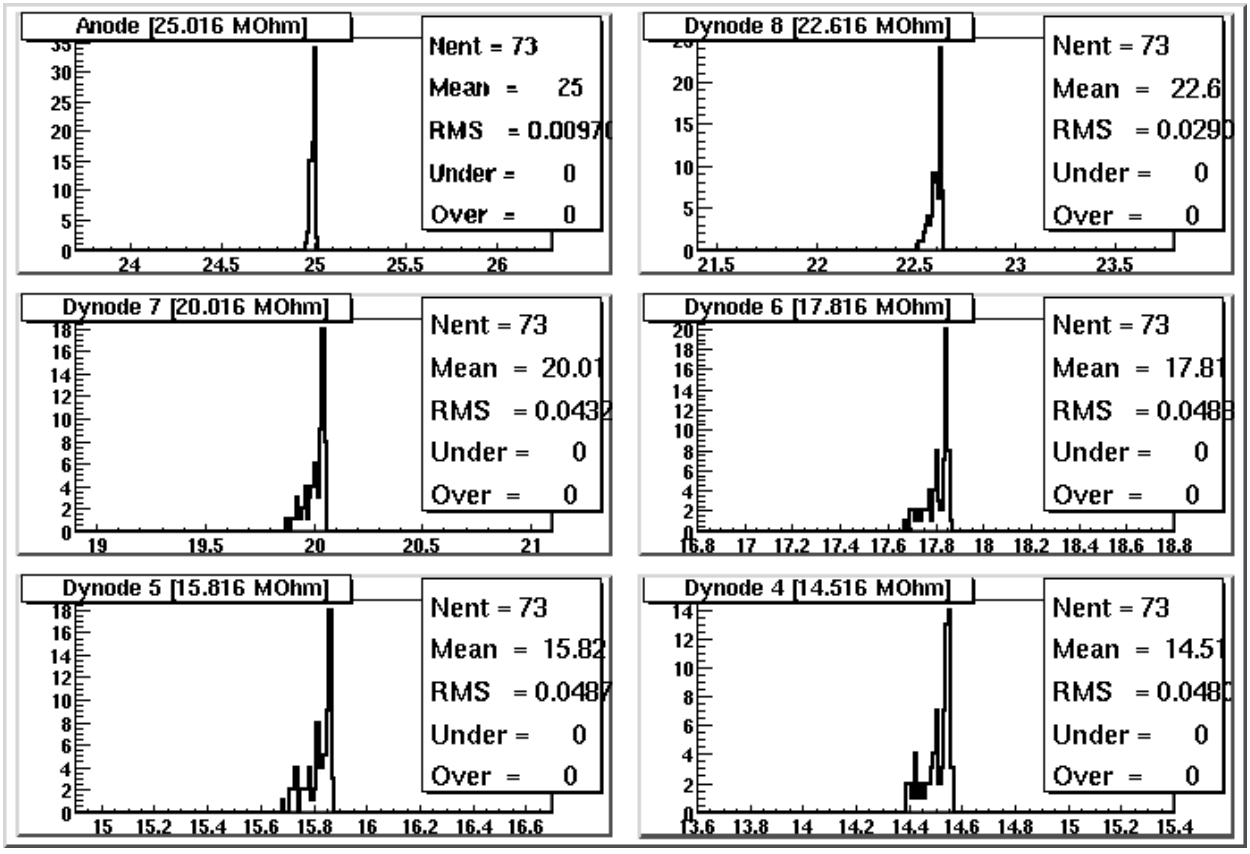
Anode [25.016 MOhm]
Nent = 73
Mean = 25
RMS = 0.0097
Under = 0
Over = 0
Dynode 8 [22.616 MOhm]
Nent = 73
Mean = 22.6
RMS = 0.029
Under = 0
Over = 0
Dynode 7 [20.016 MOhm]
Nent = 73
Mean = 20.01
RMS = 0.043
Under = 0
Over = 0
Dynode 6 [17.816 MOhm]
Nent = 73
Mean = 17.81
RMS = 0.048
Under = 0
Over = 0
Dynode 5 [15.816 MOhm]
Nent = 73
Mean = 15.82
RMS = 0.048
Under = 0
Over = 0
Dynode 4 [14.516 MOhm]
Nent = 73
Mean = 14.51
RMS = 0.048
Under = 0
Over = 0

Fig. 9

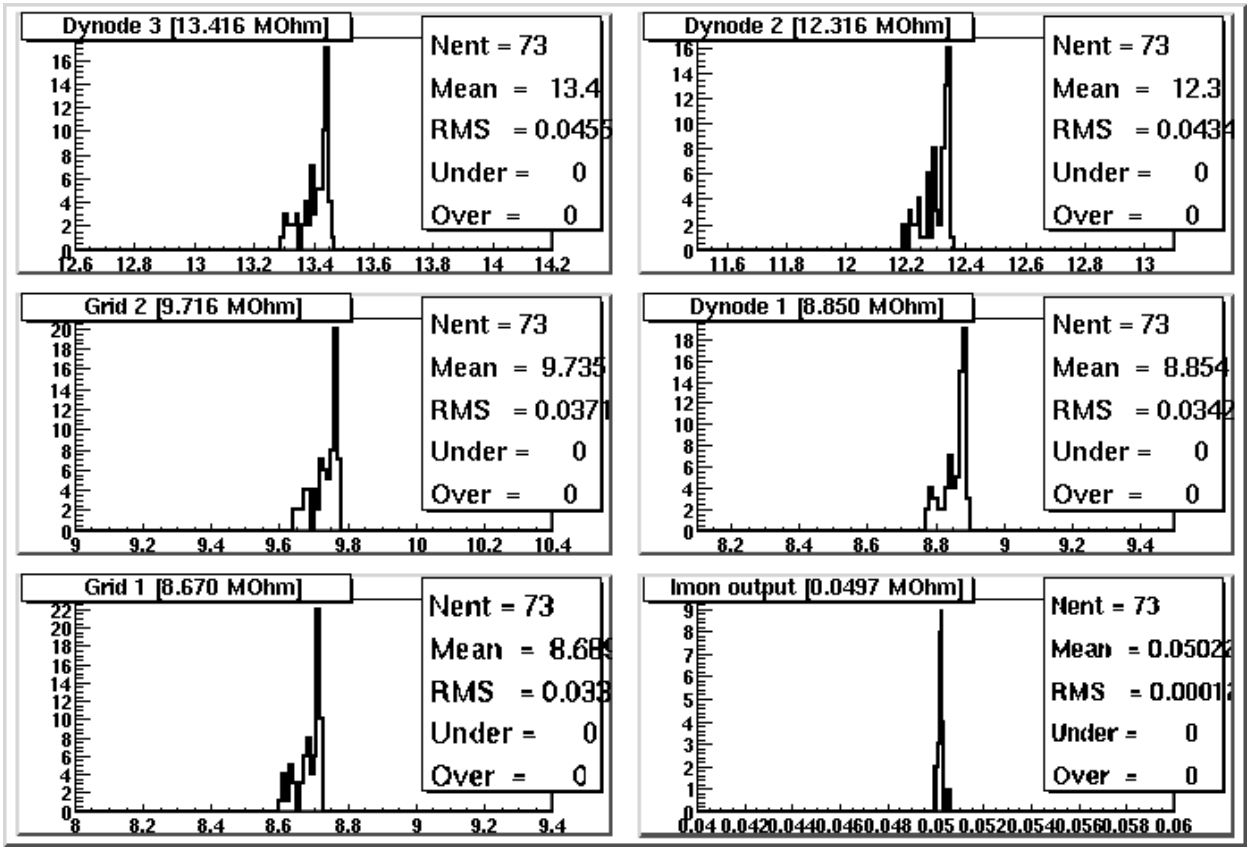
Dynode 3 [13.416 MOhm]
Nent = 73
Mean = 13.4
RMS = 0.045
Under = 0
Over = 0
Dynode 2 [12.316 MOhm]
Nent = 73
Mean = 12.3
RMS = 0.043
Under = 0
Over = 0
Grid 2 [9.716 MOhm]
Nent = 73
Mean = 9.735
RMS = 0.037
Under = 0
Over = 0
Dynode 1 [8.850 MOhm]
Nent = 73
Mean = 8.854
RMS = 0.034
Under = 0
Over = 0
Grid 1 [8.670 MOhm]
Nent = 73
Mean = 8.68
RMS = 0.033
Under = 0
Over = 0
Imon output [0.0497 MOhm]
Nent = 73
Mean = 0.0502
RMS = 0.0001
Under = 0
Over = 0

Fig. 10

The relationships: Vmon[mV] vs Vcin[mV], Imon[mV] vs Vcin[mV], HV[V] vs Vcin[mV], HV[V] vs Vmon[mV] and HV[V] vs Imon[mV] are linearly fitted in the data analysis. The coefficients p1 and p0 indicated in table 3 represent the slope and the constant term of the fitted line respectively. Figure 11 shows some examples.

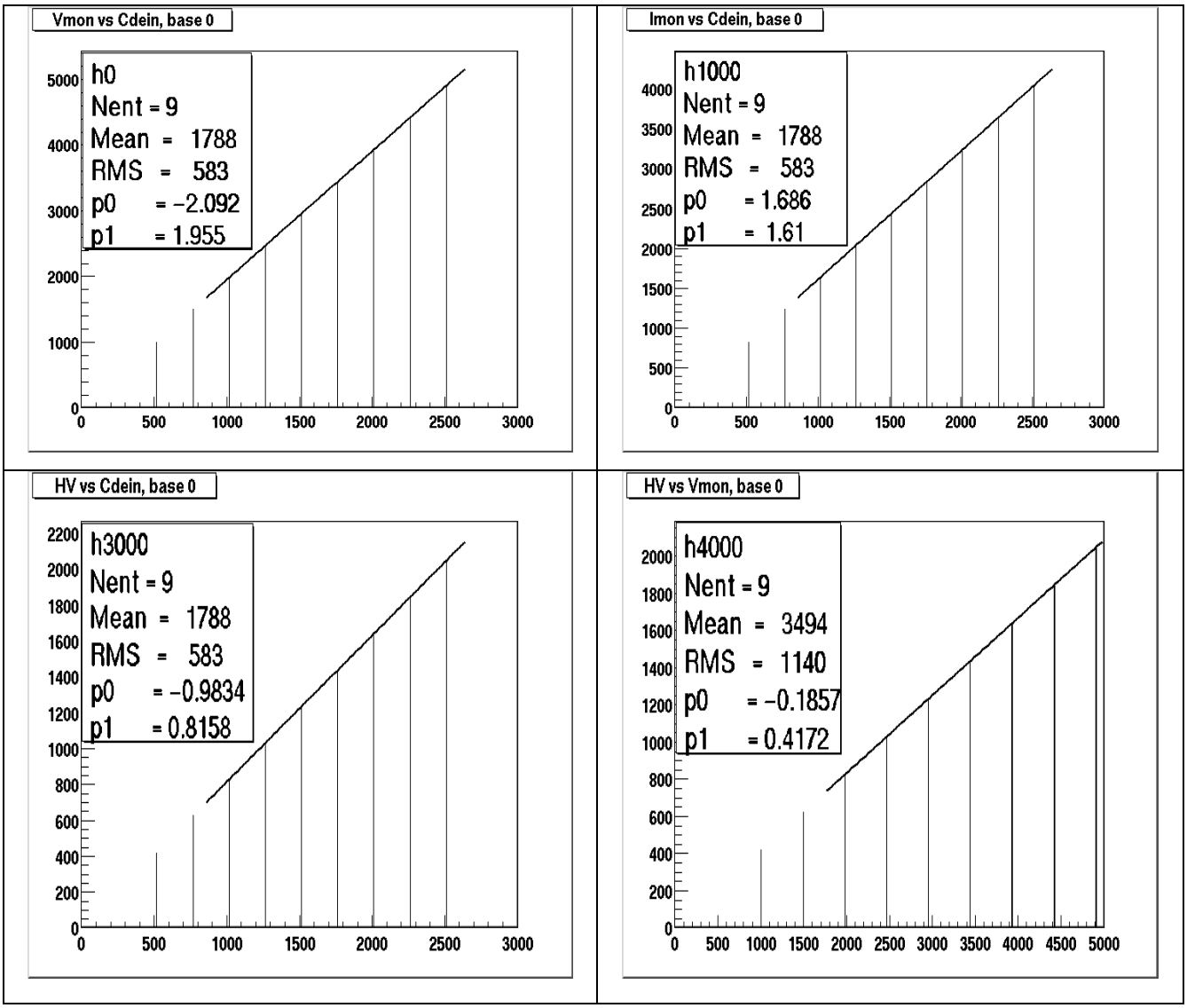

*Cdein≡Vcin

Fig.11

In fig. 12 the distributions of the fitted parameters p1 and p0 are shown . All the HVPS look very similar (the distribution widths are inside 3‰ for HV vs Vcin even around 1.5‰) suggesting the possibility of using the average values as reference values for all the bases instead of individual parameters one for each base.

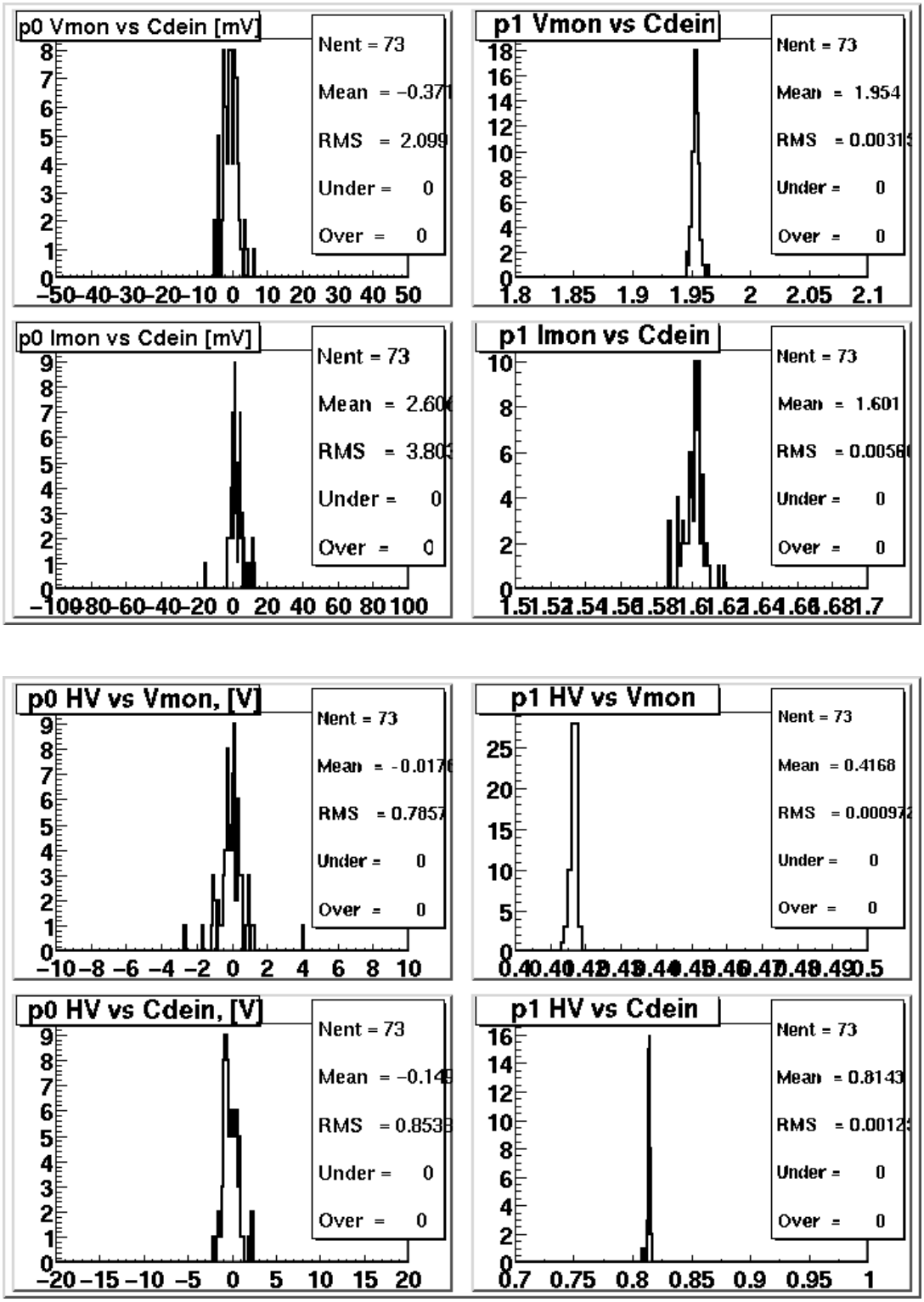

*Cdein≡Vcin

Fig .12

In fig. 13 the maximum differential non-linearity for each of the 73 pre-production bases are shown. The obtained values are in good agreement with the HVPS specifications (maximum 1 ‰).

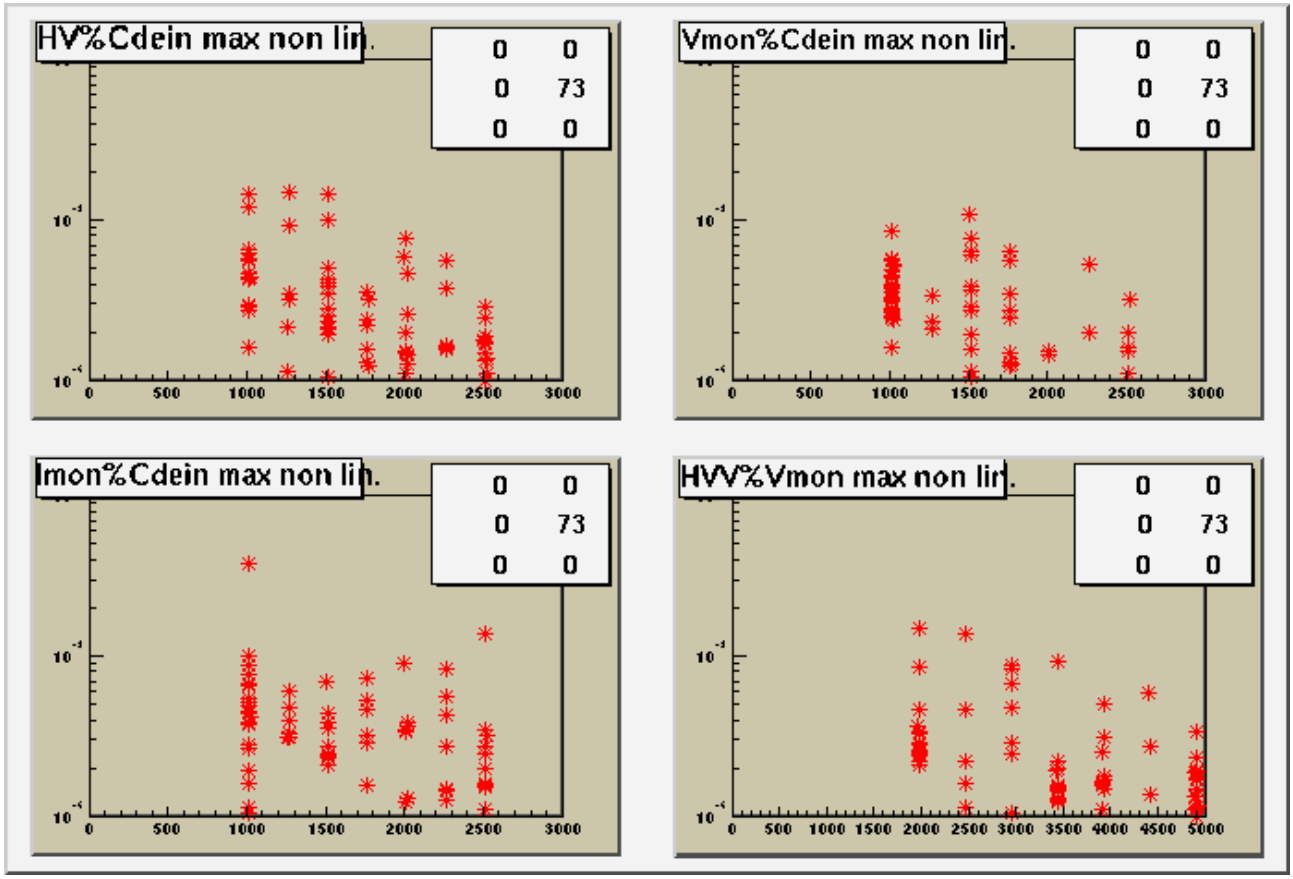

*Cdein≡Vcin

Fig. 13

The results obtained on the HVPS of the pre-production bases have been compared with data supplied by the ETL company for each HVPS. Fig. 14 shows the distribution of p0 and p1 obtained by fitting HV versus Vcin ETL data.

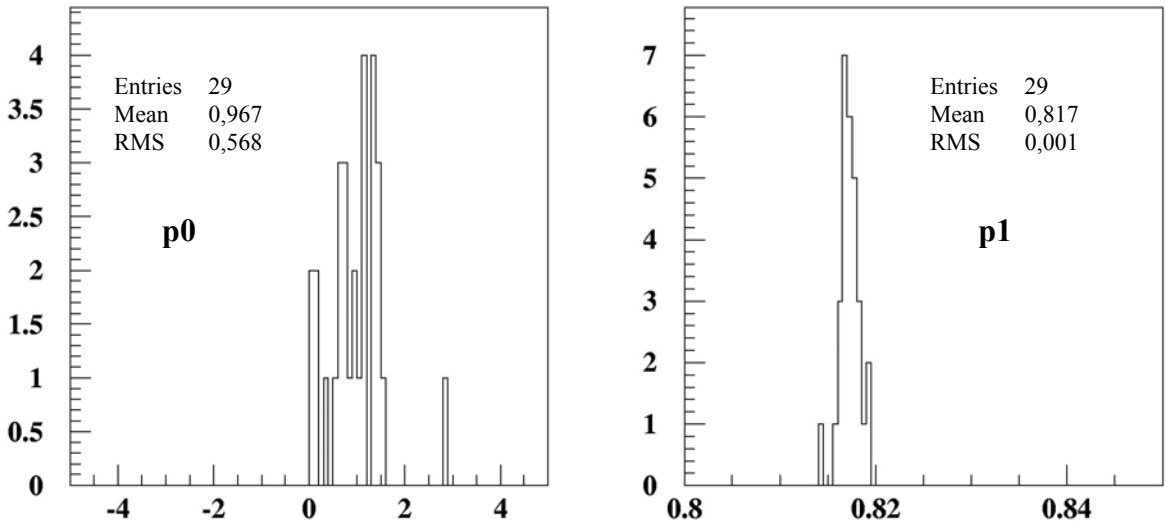

Fig. 14

The difference between the ETL data and the test bench ones is of the order of 5 ‰ as it can also be seen on fig.15.

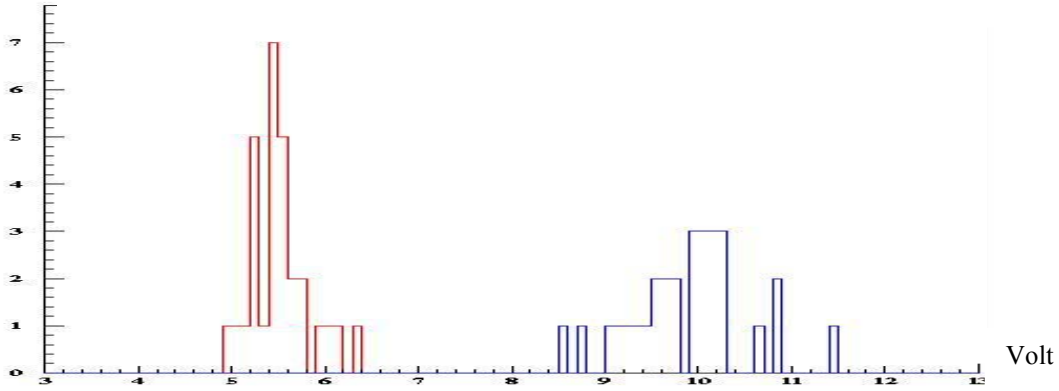

Fig 15: ΔV between HV output obtained by using the ETL fit and the test bench fit for 2 different fixed values of Vcin corresponding to 1000 V (red) and 2000 V (blue).

Fig.16 shows the distribution of the maximum HVPS power absorption measured for Vcin = 2.5V.

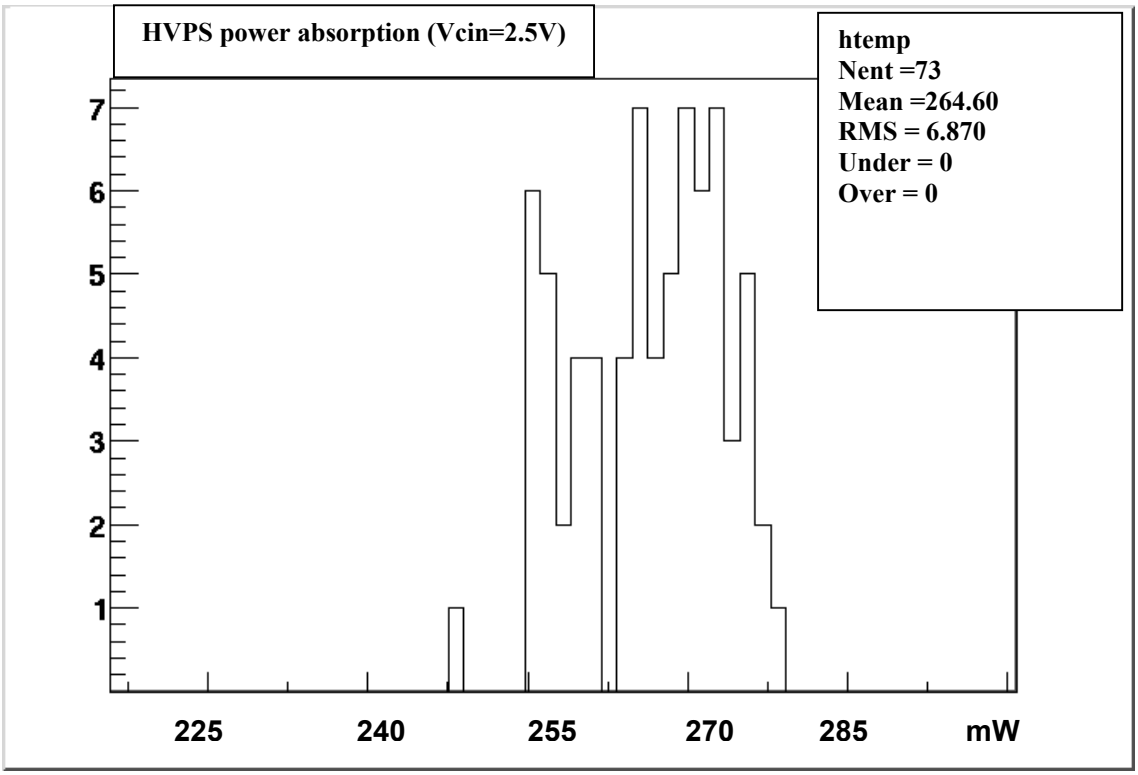

Fig. 16

The results for the buffer ratio Vo/Vi calculated on the 73 pre production bases are shown in fig 17.

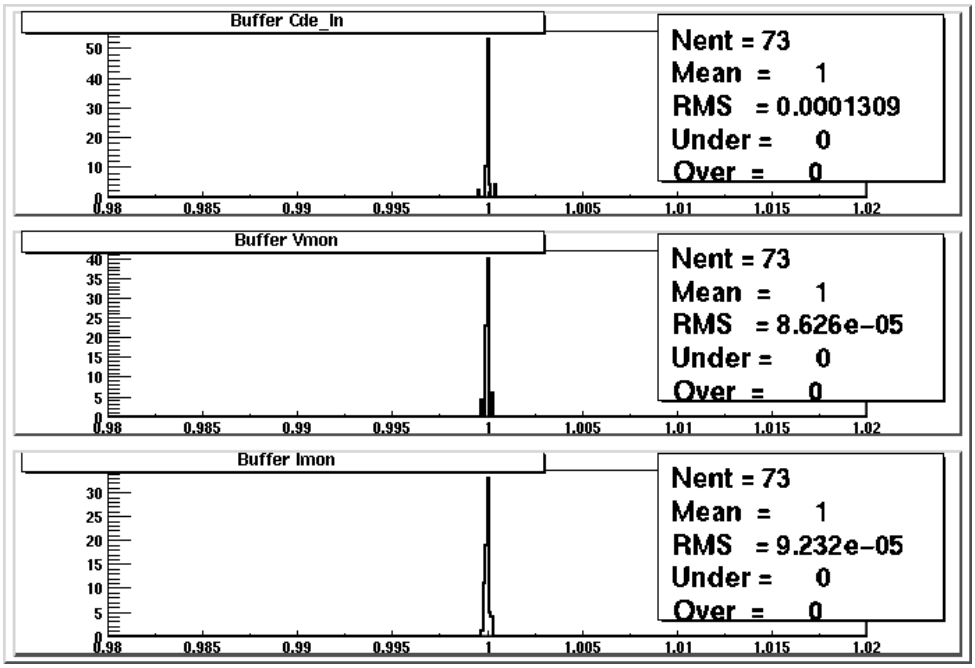

*Cdein≡Vcin

Fig. 17

Fig 18 shows the anode output as seen on a digital oscilloscope with R_{in}=1MΩ. The RC check is obtained by measuring τ on the PM6666 counter for a fixed threshold. Fig 19 shows the distribution of the τ parameter for the 73 pre-production bases.

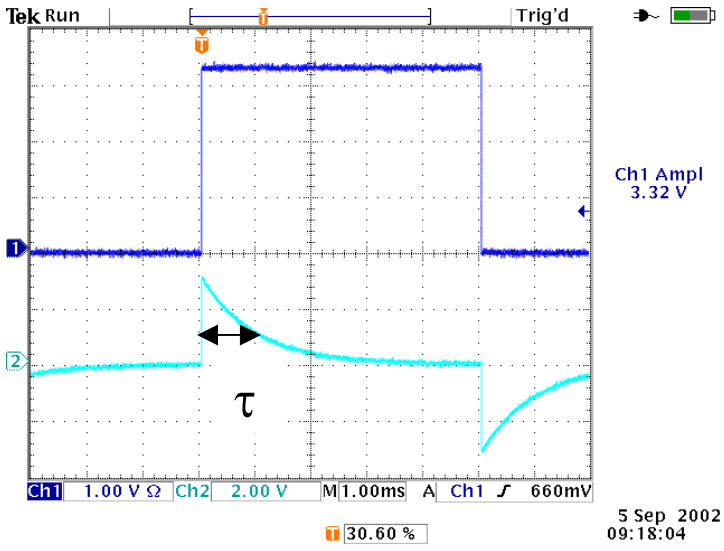

Fig. 18: anode signal as seen on the 1 MΩ input of the scope. Ch.1: input on the T11 test point. Ch.2: waveform after the RC anode.

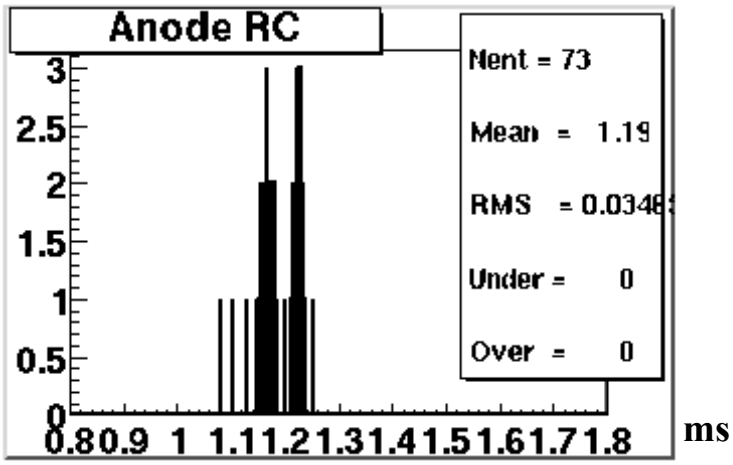

Fig. 19

In fig 20 the distribution of the amplification factor is shown. The nominal dynode amplification is 32. An average value of 27.4 has been found that is in good agreement with the simulation taking in the account the cable impedance.

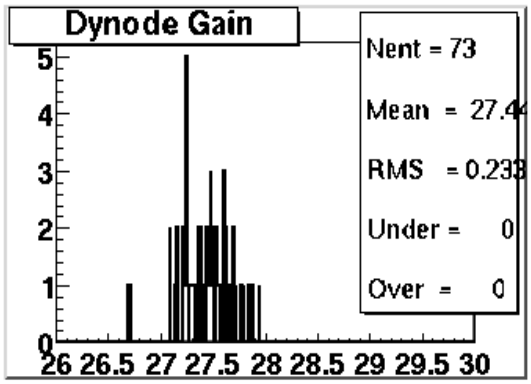

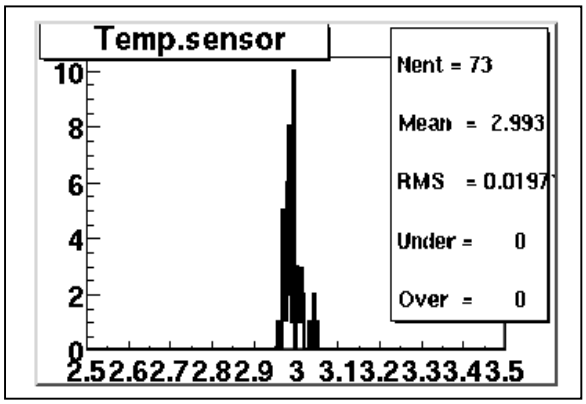

Fig. 20

Fig.21

The results obtained in testing the temperature sensor for the 73 pre-production bases are shown in Fig 21. The obtained average value is consistent with the room temperature during the tests.

7. Conclusions

A test bench and a testing procedure has been developed by INFN-TO to control the Pierre Auger Observatory – Surface Detector PMT base production. The procedure also allows the HV power supplies characterization.
Data obtained during the test of each base are sequentially stored in a file with the together results from the subsequent analysis program. This will allow to retrace the base performances at the end of the production line.
An example of the analysis program data output has been shown in Tab.2. For operative purposes a reduced set of these parameters has been sent to the collaboration for each delivered base (see Tab. 4).
A second copy of the test bench is actually operative c/o the FEDD company to test the IPN production.
The results obtained for the pre-production show a good uniformity of produced bases.

References

[1] Suomijärvi, T. for the Pierre Auger Observatory Collaboration, *Surface Detector Electronics for the Pierre Auger Observatory*, ICRC 2001, GAP-2001-026

[2] Genolini, B., Nguyen Trung, T., Pouthas, J., Lhenry-Yvon, I., Parizot, E., Suomijärvi, T., *Design of the Photomultiplier Bases for the Surface Detectors of the Pierre Auger Observatory*, IPNO DR-01-010, Institut de Physique Nucléaire d'Orsay, GAP-2001-021

[3] Genolini, B., Aglietta, M., Creusot, A., Fulgione, W, Gomez, F., Lhenry-Yvon, I., Morello, C., Navarra, G, Nguyen Trung, T., Pouthas, J., Suomijärvi, T., Vigorito, C., *Low Power High Dynamic Range Photomultiplier Bases for the Surface Detectors of the Pierre Auger Observatory*, Presented at the 2002 Beaune conference on photodetection, GAP-2002-038

[4] Aglietta, M., Fulgione, V, Gomez, F., Morello, C., Navarra, G, Vigorito, C., *The high voltage test bench: characterization of the pre-producioin modules.*, GAP –2003-021

[5] Tripathi A.,.Arisaka K., Ohnuki T., Ranin P., *Effects of Earth's Magnetic Field on Production Photonis PMTs*, GAP-2002-013

[6] Clark P. and Dye A., *Environmental stress screening and burn-in procedure for electronic equipment used within the Pierre Auger Observatory,* GAP-2002-002

Appendix A: block diagram of the system used at Neohm

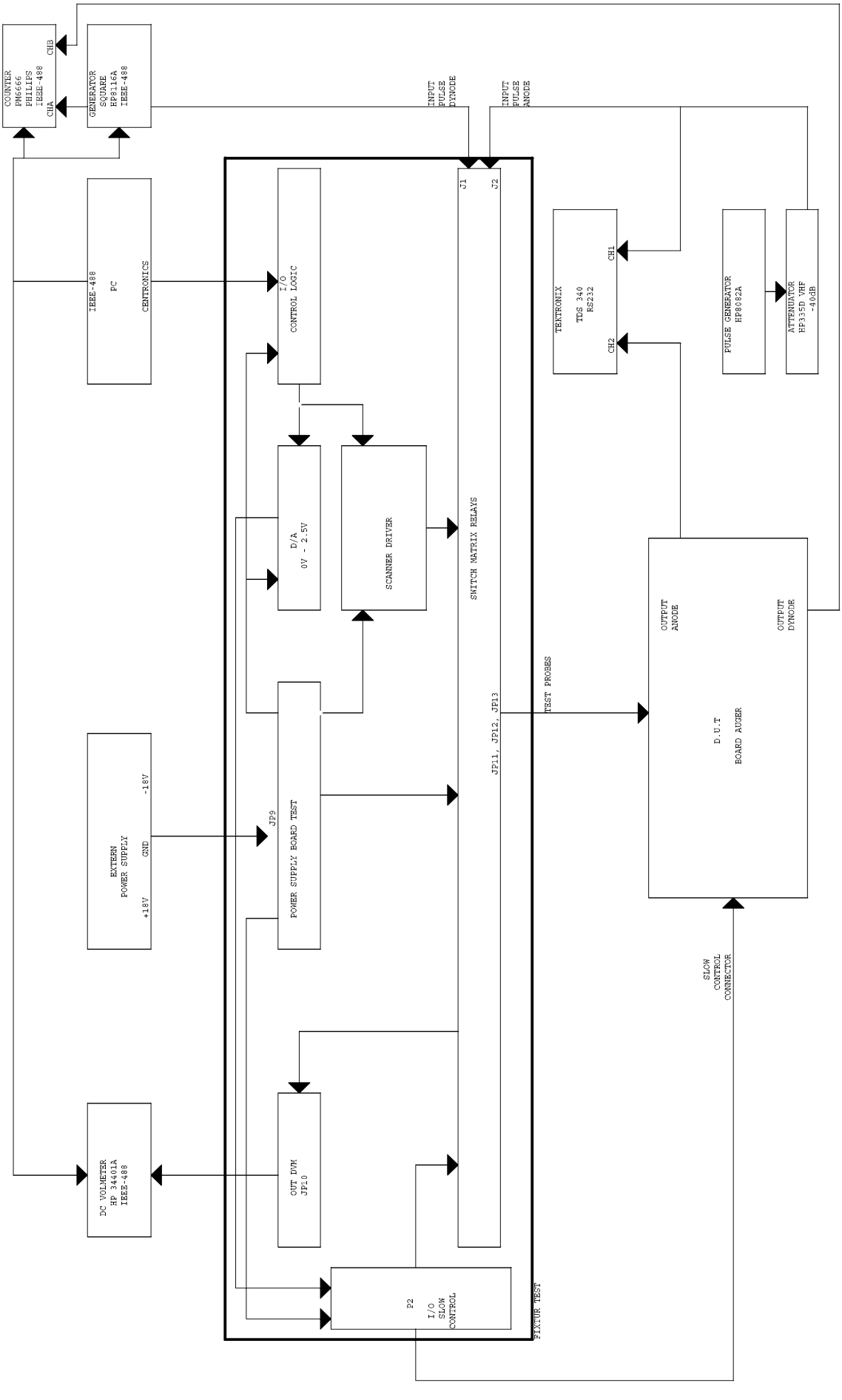

Appendix B: electrical drawing of the base (dynode voltage repartition)

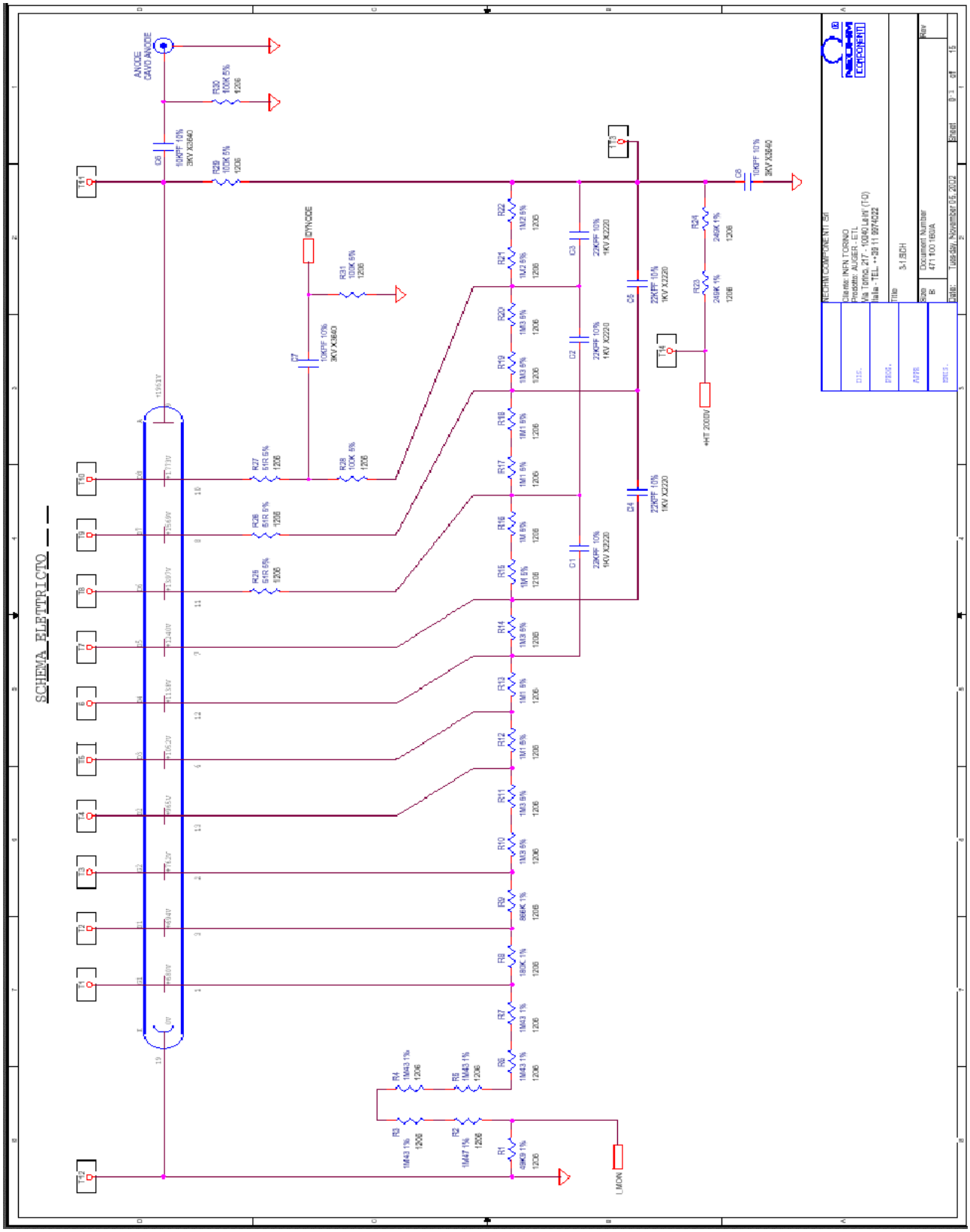

Appendix B: electrical drawing of the base (active components)